EXTENDED PDF FORMAT
SPONSORED BY

http://discover.bio-rad.com

Characterization of Excess Electrons in Water-Cluster Anions by Quantum Simulations

László Turi, *et al.*

Science **309**, 914 (2005);
DOI: 10.1126/science.1115808

The following resources related to this article are available online at www.sciencemag.org (this information is current as of July 3, 2007):

Updated information and services, including high-resolution figures, can be found in the online version of this article at:
http://www.sciencemag.org/cgi/content/full/309/5736/914

A list of selected additional articles on the Science Web sites **related to this article** can be found at:
http://www.sciencemag.org/cgi/content/full/309/5736/914#related-content

This article **cites 32 articles**, 5 of which can be accessed for free:
http://www.sciencemag.org/cgi/content/full/309/5736/914#otherarticles

This article has been **cited by** 30 article(s) on the ISI Web of Science.

This article has been **cited by** 5 articles hosted by HighWire Press; see:
http://www.sciencemag.org/cgi/content/full/309/5736/914#otherarticles

This article appears in the following **subject collections**:
Chemistry
http://www.sciencemag.org/cgi/collection/chemistry

Information about obtaining **reprints** of this article or about obtaining **permission to reproduce this article** in whole or in part can be found at:
http://www.sciencemag.org/about/permissions.dtl

Downloaded from www.sciencemag.org on July 3, 2007

Science (print ISSN 0036-8075; online ISSN 1095-9203) is published weekly, except the last week in December, by the American Association for the Advancement of Science, 1200 New York Avenue NW, Washington, DC 20005. Copyright c 2005 by the American Association for the Advancement of Science; all rights reserved. The title SCIENCE is a registered trademark of AAAS.

32. W. W. Gerberich *et al.*, *Acta Mater.* **47**, 4115 (1999).
33. A. M. Minor, J. W. Morris, E. A. Stach, *Appl. Phys. Lett.* **79**, 1625 (2001).
34. M. Chen *et al.*, *Science* **300**, 1275 (2003).
35. W. M. Vetter, M. Dudley, *J. Cryst. Growth* **260**, 201 (2004).
36. A. T. Blumenau *et al.*, *J. Phys. Condens. Matter* **14**, 12741 (2002).
37. J. P. Rino *et al.*, *Phys. Rev. B* **70**, 045207 (2004).
38. M. Ohyanagi *et al.*, *Scripta Mater.* **50**, 111 (2004).
39. I. A. Ovid'ko, *Science* **295**, 2386 (2002).
40. D. Wolf, V. Yamakov, S. R. Phillpot, A. Mukherjee, H. Gleiter, *Acta Mater.* **53**, 1 (2005).

41. We thank R. Kalia, D. Morgan, and S. Babcock for fruitful discussions and H. van Swygenhoven for valuable comments on the study. This work was partially supported by Air Force Office of Scientific Research–Defense University Research Initiative on Nanotechnology, Army Research Office Multidiciplinary University Research Initiative, Defense Advanced Research Projects Agency–Predicting Real Optimized Materials, the U.S. Department of Energy, and NSF. I.S. is supported by NSF grant DMR-0512228.

Supporting Online Material
www.sciencemag.org/cgi/content/full/309/5736/911/DC1
Materials and Methods
Fig. S1
References

4 May 2005; accepted 6 July 2005
10.1126/science.1114411

Characterization of Excess Electrons in Water-Cluster Anions by Quantum Simulations

László Turi,[1] Wen-Shyan Sheu,[2] Peter J. Rossky[3]*

Water-cluster anions can serve as a bridge to understand the transition from gaseous species to the bulk hydrated electron. However, debate continues regarding how the excess electron is bound in $(H_2O)_n^-$, as an interior, bulklike, or surface electronic state. To address the uncertainty, the properties of $(H_2O)_n^-$ clusters with 20 to 200 water molecules have been evaluated by mixed quantum-classical simulations. The theory reproduces every observed energetic, spectral, and structural trend with cluster size that is seen in experimental photoelectron and optical absorption spectra. More important, surface states and interior states each manifest a characteristic signature in the simulation data. The results strongly support assignment of surface-bound electronic states to the water-cluster anions in published experimental studies thus far.

Clusters are widely studied, both for their direct role in atmospheric and interstellar chemistry and for their intermediacy between gaseous and condensed phases, which renders them useful simplifying models for complex molecular processes in solution. Negatively charged water clusters have long been used as models to understand the hydrated electron in bulk water. Since its discovery in 1962 (*1*), the hydrated electron has been the subject of numerous experimental (*2*–*5*) and theoretical (*6*–*10*) studies for its wide-ranging role in chemical and biological electron transfer. A consistent physical picture of its structural, spectral, and dynamic properties has emerged, bolstered in part by details extracted from clusters (*11*–*26*). However, a key issue remaining with regard to the cluster data is whether the electron is bulklike, trapped in the cluster interior by oriented solvent molecules, or stabilized in a surface-bound state specific to the cluster environment. This issue bears critically on the relation of cluster observations to bulk properties and the transition from one regime to the other.

Here, we address the question through mixed quantum-classical molecular simulation, which allows the direct computation of the experimental observables for these clusters. We show that the available experimental energetic and spectral data are completely consistent with the conclusion that the anionic water clusters observed to date bind the excess electron on the surface, although the long-anticipated spontaneous transition to interior states is indicated for clusters in the range of 100 to 200 molecules.

Barnett *et al*. first identified surface states through a series of quantum mechanical simulations of negatively charged water clusters (*11*). For their model, they found that clusters comprising approximately 8 to 32 water molecules bind the excess electron preferentially in a localized state on the cluster surface. The calculations predicted transition to compact hydrated electron-like interior states with increasing cluster size ($32 < n < 64$). These observations parallel the later theoretical discovery by Berkowitz and co-workers (*27*) that polarizable atomic anions preferentially adopt surface states in clusters as well (*27*–*29*).

Experiments have provided indirect insight into the electronic structure. The comprehensive studies of photoelectron spectra in cluster-size-selected molecular beams by Coe *et. al* (*15*) led to an excellent correlation of the most probable vertical detachment energy [(VDE), the energy needed to remove an electron at the anion's geometry] with the cluster size, n, through the largest cluster measured, $n \leq 69$. For clusters of $n \geq 11$, the spectroscopic data fit well to a simple linear relationship in $n^{-1/3}$ for the size dependence, based on a dielectric model assuming interior states (*11*). Because the correlation line extrapolated to a value for the infinite cluster that was consistent with simulation of bulk solvated electrons in ambient water, the authors concluded that these clusters were consistent with hydrated electron-like interior states.

However, in an important theoretical work, Makov and Nitzan developed a continuum dielectric model to evaluate the energy and free-energy differences between solvation of a spherical ion (or electron) in the center versus on the surface of a spherical solvent cluster and also estimated the VDEs (*13*). For an ion of constant radius in a solvent with high dielectric constant, they showed that the free energy of transfer between the surface and interior of the cluster essentially vanishes. The VDE of a surface state for a negative ion was actually found to be slightly larger than for an ion at the center of the solvent shell. We note that for an electron that is expectedly more delocalized at the surface than in the interior, this difference should be compensated (or possibly overcompensated, thus reversing the VDE ordering). In addition, Makov and Nitzan showed that both interior and surface states manifest the linear scaling of the VDE with $n^{-1/3}$ seen experimentally, so that this scaling did not distinguish the excess electron-binding morphologies (*13*). Of particular importance, for the infinite cluster, both surface and interior states will therefore extrapolate to the same bulk limit. Hence, the experimental observation of an extrapolated value close to the bulk does not a priori distinguish between surface and interior states.

Later, Ayotte and Johnson (*16*) measured cluster-size-selected optical absorption spectra by photodestruction. The spectral peak positions also shift linearly with $n^{-1/3}$, consistent with an excited-state energy that also scales with cluster radius. The authors noted that the excited-state VDE slope was implicitly smaller than the ground-state slope, a result that would be in harmony with different radii for the excited and ground states. The energy gap between the ground and the excited states increased with cluster size, in accord with a contracting radius. They pointed out that, of the earlier simulated energies (*11*), those for interior states were quantitatively closer to the

---

[1] Eötvös Loránd University, Department of Physical Chemistry, Budapest 112, Post Office Box 32, H-1518, Hungary. [2] Department of Chemistry, Fu-Jen Catholic University, Taipei, Taiwan 242, ROC. [3] Department of Chemistry and Biochemistry, Institute for Theoretical Chemistry, University of Texas at Austin, Austin, TX 78712–1167, USA.

*To whom correspondence should be addressed. E-mail: rossky@mail.utexas.edu

measurements than those for surface states. Further, the spectra exhibited not only a blue shift with increasing size but also an increasing line width. The sequence of spectra appeared qualitatively consistent with a systematic evolution toward the bulk ambient spectrum.

Bartels summarized the entire controversy (*19*) and reevaluated the optical absorption spectra acquired by Ayotte and Johnson (*16*) based on dispersion relationships. Statistical moment analysis of the spectra yielding values for both the thermally averaged spatial dispersion $\langle r^2 \rangle$ and the kinetic energy $\langle T \rangle$ of the excess electron leads to a distinctive behavior with cluster size: The radius decreases strongly with increasing *n*, approaching the bulk value from above, while, in parallel, the kinetic energy approaches the bulk value from below. These quantities vary smoothly with *n*, without the discontinuity in either quantity that might indicate a transition between surface and interior states.

The latest work in the field has come from Neumark and co-workers (*22*), who measured the photoelectron spectra of larger water-cluster anions ($n \leq 150$) for clusters generated with both low and high backing pressures, the latter yielding presumably colder clusters. This study raised the question of temperature dependence directly, although Barnett and co-workers had provided a limited consideration (*11*) and Johnson had noted that cluster temperature is a function of preparation method and cluster size (*16*). We note that the uniform continuum model has only a weak temperature dependence. Neumark's group observed a new feature in the photoelectron spectra in colder clusters, with significantly smaller VDEs than those found by Coe *et al.* (*15*). Because of the smaller VDE, they attributed the new peaks to the presence of surface states and concluded that the earlier work had, therefore, observed interior states.

Here, we report a series of mixed quantum-classical, fully molecular simulations on $(H_2O)_n^-$ clusters with $n = 20$, 30, 45, 66, 104, and 200 and with internal kinetic energies consistent with three different temperatures, 100 K, 200 K, and 300 K. The simulation methods are described in more detail elsewhere (*6*, *8*, *10*, *30*). The water molecules are described classically, interacting through a flexible three-site potential, whereas the electron is represented by its wave function in a plane-wave basis evenly distributed on a 32- by 32- by 32-point grid. The water-electron interaction is modeled by a recent approximate pseudopotential model (*10*). Sampling is done by molecular dynamics. The water molecules evolve under the combined influence of other classical molecules and the electron. The nuclear evolution is adiabatic; the electron remains in its ground state. All the cluster simulations have been initiated from interior states of previous hydrated electron simulations (*10*). The equilibration of the systems has included tests to specifically establish that the surface states result from spontaneous migration from an interior state to the cluster surface state.

In this work, we have not attempted to evaluate the relative free energies of surface and interior states. Thus, in the ensuing discussion, "stability" refers simply to the persistence of that state over the duration of the simulation. The data reported here have been obtained from equilibrated trajectories of 30- to 80-ps length. These durations are approximately an order of magnitude longer than those of Barnett and co-workers (*11*). The present method employs several approximations, including the use of classical nuclei, the neglect of explicit solvent polarizability, and the use of an approximate electron-water pseudopotential, which neglects electron-solvent dispersion interactions (*23*). Simulations using the same set of approximations for the bulk hydrated electron give results that are consistent with experiments (*10*). Because these approximations are expected to introduce significant quantitative error for smaller clusters (*23*), we consider only $n \geq 20$ here. In particular, the use of the present water model's fixed charge polarization, appropriate to the bulk liquid environment, is likely to overestimate the molecular dipole in a small cluster and, correspondingly, artificially enhance the electrostatic electron binding. Spectral results on the hydrated electron at low bulk density and high temperature (*31*) indicate that models like those used here are correspondingly limited in that regime.

The electronic distributions for the ground-state anions fall in two distinct categories. Identification follows from the radius of the cluster r_c, the electron radius [radius of gyration, $r_e = \langle r^2 \rangle^{1/2}$], and the distance between the centers of the electron and water distributions *R*. An interior state is localized within the cluster, so that $R + r_e < r_c$. For a surface state, $R \sim r_c$, and significant electronic amplitude appears outside the nominal cluster radius (Fig. 1). It is notable that the surface electronic states are highly analogous to bulk hydrated electron distributions (*6*), with typical *s* and *p* character. At 200 K and 300 K, we find that only the $n = 200$ cluster exhibits a stable interior electronic state; smaller clusters ($n = 20$, 30, 45, 66, and 104) support stable surface states. At 100 K, only the smallest clusters, up to $n = 45$, spontaneously manifest the excess electron on the surface. Larger clusters, and an alternative $n = 45$ configuration, are stable with the electron in an interior state. However, this may be a kinetic effect, and we cannot conclude from this that the lower temperature favors interior states.

The validity of these calculations can be tested with the computed physical properties of the clusters, such as absorption spectra at different temperatures (Fig. 2). The spectral evolution of the surface-state clusters, in terms of both shift and width, completely parallels the experimental spectra of Ayotte and Johnson (*16*). There is only weak temperature dependence for surface states. The experimental spectral trends should therefore be substantially the same over a very wide range of cluster temperatures, as long as the electron is surface bound.

In contrast, the spectrum at 300 K for the $n = 200$ interior state is nearly identical to the bulk hydrated electron spectrum (*10*). At 200 K, the corresponding $n = 200$ spectrum is slightly blue-shifted from the bulk peak center at 298 K (*10*). At 100 K, the spectral evolution exhibits a sharp shift at the point of surface to interior transition (at $n \approx 45$), and at $n = 200$ is blue-shifted by nearly 0.5 eV from the bulk simulated spectrum at 298 K (*10*). This characteristic blue-shift from the bulk spectrum would be an experimental signature of cold interior states. We attribute the temperature dependence of the interior state clusters to solvent contraction (electrostriction) around the electron with decreasing temperature. For surface states, a contraction of solvent does not increase confinement of the electron. For the bulk hydrated electron, simulations (*32*) with the same model used here (*10*) have qualitatively reproduced the experimental temperature dependence of spectra in the liquid and shown that at liquid densities, this dependence lies predominantly, although not entirely (*31*), in the solvent density response.

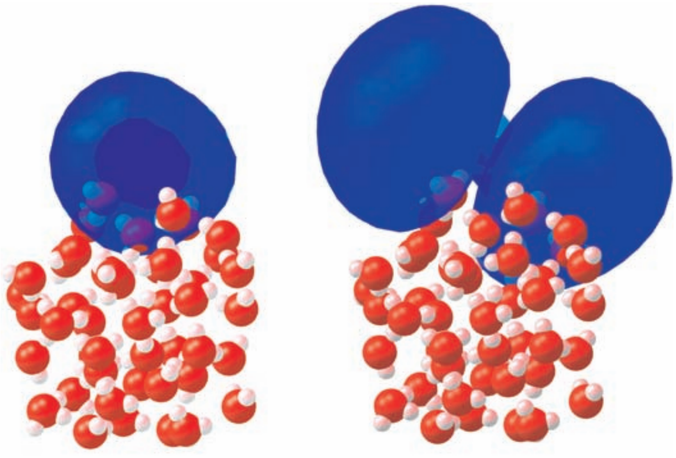

Fig. 1. Typical electronic distributions for the surface state of $(H_2O)_{45}^-$. (Left) Ground state, isosurface enclosing 80% of electron density, with inner shadow isosurface at 30%. (Right) Excited state, isosurface enclosing 80% of electron density.

The temperature dependence observed here contradicts the conclusions in the seminal simulations of Barnett *et al.* (*11*, *12*); the discrepancy is likely due to the difference in model and/or the limited sampling accessible in the older work. Our low-temperature spectra do appear qualitatively similar to those of Barnett *et al.* (*12*) except for the size dependence. As noted, the surface to interior transition occurred there between $n = 32$ and 64 at 300 K (*11*), whereas our model predicts a transition in the $104 < n < 200$ range.

The calculated spectra shown in Fig. 2 broaden and shift to the blue with increasing cluster size, in excellent agreement with experiments. The blue shift results from a sharper increase in stabilization of the *s* state than of the more diffuse *p* state as the cluster grows. The broadening is assignable primarily to an increasing *p*-state splitting. For smaller clusters, the *p* states are more nearly degenerate in each configuration, leading to overall narrower spectra.

Extrapolation of the calculated spectral maxima energies and vertical detachment energies to infinite cluster size is compared in Fig. 3 with the extrapolations of analogous experimental data from Coe (*15*) and Johnson (*16*). Because the surface states exhibit only weak temperature dependence, the surface-state points in the plot are averaged over the temperatures simulated. The simulated surface-state data follow a slope similar to the experiments. Also, as in experiments (*16*), the ground-state energy (VDE) slope is different from that for the excited state, and, correspondingly, both lines extrapolate to very near the ambient bulk values for the model. This result is expected based on the continuum dielectric model (*13*). In contrast, the simulated interior-state data clearly differ from experimental data, and the low-temperature data do not extrapolate to room-temperature bulk properties. If the surface-state to interior-state transition does occur above $n = 104$, we find that the observed results of Coe (*15*) and Johnson (*16*) would then be consistent with our simulated results over a wide range of actual cluster temperatures.

Comparison of the calculated radius of gyration and kinetic energy data with experimental data makes an even more compelling case than the spectral data for predominance of surface states (Fig. 4). The distinct trends with cluster size follow the experimentally derived size dependence (*19*) faithfully [see figure 1 in (*19*)]. The radius smoothly approaches the bulk value from above as the clusters grow, whereas the interior states have nearly identical radii. A similar pattern holds for the kinetic energy; the trend follows experimentally derived size dependence (*19*). The interior states have much higher kinetic energy than the surface states. There is some increase with decreasing temperature, but all interior-state kinetic energies are similar to the large cluster limit. These trends are qualitatively similar to those seen originally by Barnett (*11*), although different in magnitude.

Some additional insight into the regularity of the behavior of the surface-state clusters can be obtained by computing the mean dipole polarization, $\langle\mu\rangle$, of the molecular clusters in the direction of the electronic center of charge. The surface states manifest a variation of $\langle\mu\rangle$ in the 15 to 33 Debye range, for $20 < n < 104$ cluster sizes at 200 K, with a nearly linear dependence on $n^{-1/3}$, in accord with the expected size dependence of the Makov-Nitzan dielectric model (*13*). This molecular-cluster dipole moment largely compensates the dipole associated with the position of the surface-bound electron with respect to the cluster center of mass.

There are quantitative shortcomings in the calculated values compared with experimental reports. The calculated VDE values are closer to those only recently measured by Neumark (*22*)

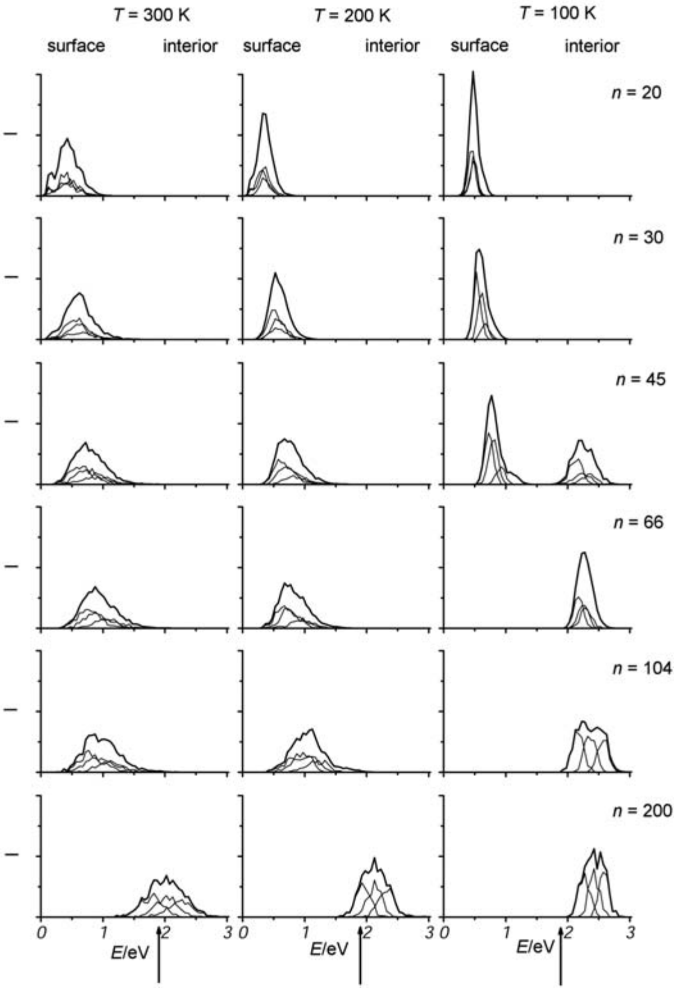

Fig. 2. Optical absorption spectra for $(H_2O)_n^-$ clusters at kinetic energies characteristic of three different temperatures, 300 K, 200 K, and 100 K. The first three subbands of each spectrum are also indicated (curves within envelope). The arrows at the bottom indicate the simulated bulk hydrated electron spectral maximum for the same model at 298 K (*10*). The trend with *n* of surface-state spectra follows that observed in the experimental spectra [see figure 2 in (*16*)].

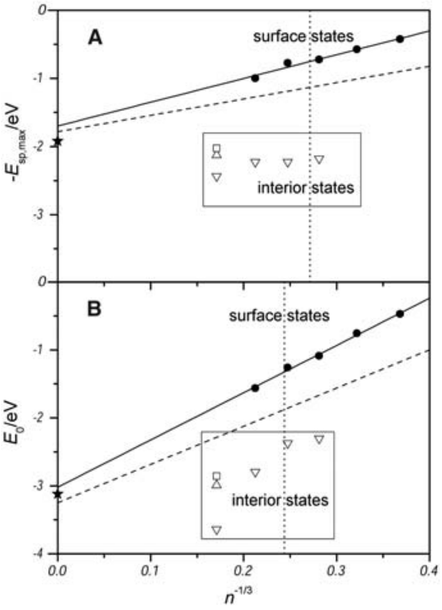

Fig. 3. Simulated spectral maxima for optical absorption (A) and mean VDEs (B) for $(H_2O)_n^-$. The surface-state data (filled circles) are reported as the average over all temperatures studied. All data for the interior states (open symbols) fall in the highlighted rectangular area. ▽, 100 K; △, 200 K; □, 300 K. The bold stars at $n^{-1/3} = 0$ indicate the simulated bulk hydrated electron values at 298 K (*10*). The linear fits derived from the VDE data from Coe and Bowen (*15*) and the spectral maxima of Ayotte and Johnson (*16*) are also shown (dashed lines). The vertical dotted lines indicate the maximum experimental cluster sizes reported in (*15*) and (*16*). The linear extrapolation of the simulations is very similar to that seen in experiments [see figure 3 in (*16*)].

for the identified surface states (denoted there as Isomer II) than to the Coe data (*15*) considered here. However, the surface and interior electron-binding morphologies lead to distinctly different trends in measured physical properties: vertical detachment energy, optical absorption spectra, kinetic energy, and electronic radius. The comparison of the trends to the corresponding published experimental data strongly supports the conclusion that the available experiments reporting these results reflect only clusters characterized by electronic surface states. The newly reported species associated with more weakly bound electrons (*22*) are presumably also surface states, as concluded in that report, but they do not appear to be a simple extrapolation of those found here. We have carried out a set of preliminary simulations that show that electrons attached to already formed very cold water clusters produce surface-state species with a range of vertical electronic detachment energies of magnitudes well below those of the clusters simulated here. We therefore speculate that the surface states recently observed are the result of such attachment processes. The differences may reflect alternative proton-ordering motifs, as suggested by Johnson and co-workers (*25*, *26*).

Our findings substantially support the physical picture originally put forth by Barnett and co-workers (*11*) and strongly suggest that for larger clusters than observed to date, the transition to an interior state should occur. Most important, the results indicate that both the physical state and cluster temperature of interior states can be characterized from optical spectra or from the character of the high-energy end (VDE > 3.0 eV) of photoelectron spectra.

These results reinforce the conclusion that simple continuum dielectric models of these clusters have considerable power, particularly for surface states, but are limiting in describing the temperature dependence of the spectra and kinetic energy, key factors in the interpretation of data for interior states. The weak temperature sensitivity of surface states clearly explains why extrapolation of the surface-state properties leads to a value close to the bulk ambient VDE, because this bulk state is nearly isoenergetic with the actual extrapolation limit, the semi-infinite solvent surface state (*13*). The relatively large temperature dependence of interior-state properties also emerges as a convenient way to distinguish the two binding morphologies. Finally, we note that nuclear quantum effects on water structure will play a role in the quantitative comparison of experiments and simulations. Classical water clusters are expected to exhibit the characteristics of significantly colder systems when considered at the same nominal temperature as experimental (quantized) water clusters (*8*, *33*).

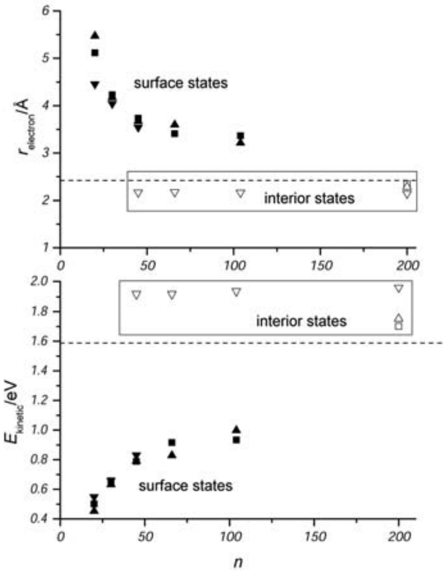

Fig. 4. Radius of gyration and kinetic energy of the excess electron in water-cluster anions at three simulation temperatures, 100 K (▽), 200 K (△), and 300 K (□). Filled symbols denote surface states, open symbols denote interior states. The dashed lines show the simulated radius of gyration and kinetic energy of the hydrated electron in bulk water at 298 K (*10*). The surface-state data behave comparably to the experimental data [see figure 1 in (*19*)].

References and Notes

1. E. J. Hart, J. W. Boag, *J. Am. Chem. Soc.* **84**, 4090 (1962).
2. A. Migus, Y. Gauduel, J. L. Martin, A. Antonetti, *Phys. Rev. Lett.* **58**, 1559 (1987).
3. F. H. Long, H. Lu, K. B. Eisenthal, *Phys. Rev. Lett.* **64**, 1469 (1990).
4. C. Silva, P. K. Walhout, K. Yokoyama, P. F. Barbara, *Phys. Rev. Lett.* **80**, 1086 (1998).
5. M. J. Tauber, R. A. Mathies, *J. Am. Chem. Soc.* **125**, 1394 (2003).
6. P. J. Rossky, J. Schnitker, *J. Phys. Chem.* **92**, 4277 (1988).
7. A. Wallqvist, G. Martyna, B. J. Berne, *J. Phys. Chem.* **92**, 1721 (1988).
8. B. J. Schwartz, P. J. Rossky, *J. Chem. Phys.* **101**, 6902 (1994).
9. A. Staib, D. Borgis, *J. Chem. Phys.* **103**, 2642 (1995).
10. L. Turi, D. Borgis, *J. Chem. Phys.* **117**, 6186 (2002).
11. R. N. Barnett, U. Landman, C. L. Cleveland, J. Jortner, *J. Chem. Phys.* **88**, 4429 (1988).
12. R. N. Barnett, U. Landman, G. Makov, A. Nitzan, *J. Chem. Phys.* **93**, 6226 (1990).
13. G. Makov, A. Nitzan, *J. Phys. Chem.* **98**, 3459 (1994).
14. H. Haberland, H. G. Schindler, D. R. Worsnop, *Ber. Bunsenges. Phys. Chem.* **88**, 270 (1984).
15. J. V. Coe *et al.*, *J. Chem. Phys.* **92**, 3980 (1990).
16. P. Ayotte, M. A. Johnson, *J. Chem. Phys.* **106**, 811 (1997).
17. P. Ayotte *et al.*, *J. Chem. Phys.* **110**, 6268 (1999).
18. J. V. Coe, *Int. Rev. Phys. Chem.* **20**, 33 (2001).
19. D. M. Bartels, *J. Chem. Phys.* **115**, 4404 (2001).
20. A. E. Bragg, J. R. R. Verlet, A. Kammrath, O. Cheshnovsky, D. M. Neumark, *Science* **306**, 669 (2004).
21. D. H. Paik, I.-R. Lee, D.-S. Yang, J. S. Baskin, A. H. Zewail, *Science* **306**, 672 (2004).
22. J. R. R. Verlet, A. E. Bragg, A. Kammrath, O. Cheshnovsky, D. M. Neumark, *Science* **307**, 93 (2005).
23. F. Wang, K. D. Jordan, *Annu. Rev. Phys. Chem.* **54**, 367 (2003).
24. K. D. Jordan, *Science* **306**, 618 (2004).
25. N. I. Hammer *et al.*, *Science* **306**, 675 (2004).
26. N. I. Hammer, J. R. Roscioli, M. A. Johnson, *J. Phys. Chem. A*, in press.
27. L. S. Sremaniak, L. Perera, M. L. Berkowitz, *J. Phys. Chem.* **100**, 1350 (1996).
28. G. H. Peslherbe, B. M. Ladanyi, J. T. Hynes, *Chem. Phys.* **258**, 201 (2000).
29. P. Jungwirth, D. J. Tobias, *J. Phys. Chem. B* **106**, 6361 (2002).
30. F. A. Webster, P. J. Rossky, R. A. Friesner, *Comput. Phys. Commun.* **63**, 494 (1991).
31. D. M. Bartels, K. Takahashi, J. A. Cline, T. W. Marin, C. D. Jonah, *J. Phys. Chem. A* **109**, 1299 (2005).
32. C. Nicolas, A. Boutin, B. Lévy, D. Borgis, *J. Chem. Phys.* **118**, 9689 (2003).
33. H. Gai, G. K. Schenter, L. X. Dang, B. C. Garrett, *J. Chem. Phys.* **105**, 8835 (1996).
34. This work was supported by research grants to L.T. from the Bolyai Research Fellowship, the Foundation for Hungarian Higher Education and Research, Ministry of Education, Hungary (0140/2001), and from the National Research Fund of Hungary (OTKA, T049715); by grants to P.J.R. from the U.S. National Science Foundation (CHE 0134775) and the R. A. Welch Foundation (F-0019); and by a grant to W.S.S. from the National Science Council, ROC (NSC 93-2113-M-030-006). We thank C. Lopez for his assistance in preparing Fig. 1.

7 June 2005; accepted 8 July 2005
10.1126/science.1115808

Probing the Ultrafast Charge Translocation of Photoexcited Retinal in Bacteriorhodopsin

S. Schenkl,[1] F. van Mourik,[1] G. van der Zwan,[2]
S. Haacke,[1*] M. Chergui[1]†

The ultrafast evolution of the electric field within bacteriorhodopsin was measured by monitoring the absorption changes of a tryptophan residue after excitation of retinal. The Trp absorption decreases within the first 200 femtoseconds and then recovers on time scales typical for retinal isomerization and vibrational relaxation. A model of excitonic coupling between retinal and tryptophans shows that the signal reflects a gradual rise of the retinal difference dipole moment, which precedes and probably drives isomerization. The results suggest an intimate connection between the progressive dipole moment change and the retinal skeletal changes reported over the same time scale.

In photobiology, light-induced redistributions of charge determine the dynamic force fields at all time scales and drive the structural changes needed for biological function (*1*). Photoisomerization in retinal proteins is an example in this respect. Franck-Condon excitation of all-